

Lloyd et al. – *CuticleTrace: A toolkit for capturing leaf epidermal cell shapes*

1 **CuticleTrace: A toolkit for capturing cell outlines of leaf cuticle with**
2 **implications for paleoecology and paleoclimatology**

3
4 Benjamin A. Lloyd^{1,2}, Richard S. Barclay³, Regan E. Dunn^{4,5}, Ellen D. Currano⁶, Ayuni I.
5 Mohamaad^{6,7}, Kymbre Skersies⁶, and Surangi W. Punyasena⁸.

6
7 ¹Department of Earth and Space Sciences, University of Washington, Johnson Hall Rm-070, Box
8 351310, 4000 15th Avenue NE, Seattle, WA 98195-1310;

9
10 ²Smithsonian Environmental Research Center, Smithsonian Institution, 647 Contees Wharf Road,
11 Edgewater, MD, 21037-0028;

12
13 ³Department of Paleobiology, National Museum of Natural History, Smithsonian Institution, 1000
14 Madison Drive NW, Washington, D.C. 20560;

15
16 ⁴La Brea Tar Pits & Museum, Natural History Museums of Los Angeles County, 5801 S. Wilshire Blvd,
17 Los Angeles, CA 90036;

18
19 ⁵Department of Earth Sciences, University of Southern California, 3551 Trousdale Parkway, Los
20 Angeles, CA 90089

21
22 ⁶Department of Botany, University of Wyoming, 1000 E. University Ave., Laramie, WY 82071;

23
24 ⁷Department of Geological Sciences, University of Florida, 241 Williamson Hall, PO Box 112120,
25 Gainesville, FL 32611-2120;

26
27 ⁸Department of Plant Biology, University of Illinois at Urbana-Champaign, 139 Morrill Hall, 505 South
28 Goodwin Avenue, Urbana, IL 61801.

30
31 **Authors for correspondence:**

32 Benjamin A. Lloyd; Email: blloyd96@uw.edu

33 Surangi W. Punyasena; Email: spunya1@illinois.edu

34
35 **Manuscript received _____; revision accepted _____.**

36
37 **Word count (main text): 2,402**

Lloyd et al. – *CuticleTrace: A toolkit for capturing leaf epidermal cell shapes*

41 ABSTRACT

42 **Premise:** Leaf epidermal cell morphology is closely tied to plants' evolutionary histories and
43 growth environments, and is therefore of interest to many plant biologists. However, cell
44 measurement can be time-consuming and restrictive with current methods. CuticleTrace is a
45 suite of FIJI and R-based functions that streamlines and automates the segmentation and
46 measurement of epidermal pavement cells across a wide range of cell morphologies and image
47 qualities.

48 **Methods and Results:** We evaluated CuticleTrace-generated measurements against those from
49 alternate automated methods and expert and undergraduate hand-tracings across a taxonomically
50 diverse 50-image dataset of variable image qualities. We observed ~93% statistical agreement
51 between CuticleTrace and expert hand-traced measurements, outperforming alternate methods.

52 **Conclusions:** CuticleTrace is broadly applicable, modular, and customizable, and integrates data
53 visualization and cell shape measurement with image segmentation, lowering the barrier to high-
54 throughput studies of epidermal morphology by vastly decreasing the labor investment required
55 to generate high-quality cell shape datasets.

56

57

58 KEYWORDS

59 Cell shape, high-throughput phenotyping, image processing, image segmentation, leaf area
60 index, leaf epidermis, paleobotany, paleoecology.

Lloyd et al. – *CuticleTrace: A toolkit for capturing leaf epidermal cell shapes*

61 INTRODUCTION

62 The accurate, consistent, and efficient characterization of the leaf epidermis is key to
63 advancing our understanding of the relationships of plants to their environments and
64 evolutionary histories. The morphology and arrangement of leaf epidermal cells varies
65 significantly across different environmental conditions and taxonomic groups (Kürschner, 1997;
66 Royer, 2001; Vőfély et al., 2019). These relationships have been used to constrain
67 paleoenvironmental conditions such as atmospheric CO₂ concentration (McElwain and
68 Chaloner, 1996; Royer, 2001) and canopy structure (Dunn et al., 2015; Bush et al., 2017;
69 Milligan et al., 2021), and to enhance taxonomic resolution of paleofloras (e.g. Strömberg,
70 2011). In crop science, phenomics links high-throughput phenotyping of leaf epidermal
71 characters (cell size, shape, number, etc.) with genomics to breed plants with idealized
72 physiological traits (Zhao et al., 2019).

73 Efforts to automate leaf epidermal measurement have met differing levels of success.
74 Stomata can be efficiently identified from microscope images (e.g., Fetter et al., 2019; Li et al.,
75 2022), but the accurate characterization of epidermal pavement cell morphologies remains
76 limited to specific taxa or imaging techniques (Möller et al., 2017; Li et al., 2022). As a result,
77 hand-tracing has remained the most viable option for characterizing epidermal pavement cell
78 morphology in most cases (e.g., Vőfély et al., 2019; Brown and Jordan, 2023). However, hand-
79 tracing is a slow and tedious process, with cell-outline quality highly dependent upon both the
80 tools used for tracing (e.g., mouse, stylus, tablet, desktop computer) and the experience level and
81 conscientiousness of the tracer. The high labor requirement of hand tracing—and the non-
82 standardized measurements that result—imposes a barrier to the use of cell shape in multiple
83 disciplines. Regardless, hand-traced datasets have been part of high-impact studies studying cell

Lloyd et al. – *CuticleTrace: A toolkit for capturing leaf epidermal cell shapes*

84 shape, growth environment, and evolutionary history (Dunn et al., 2015; Bush et al., 2017;
85 Vőfély et al., 2019). These studies demonstrate how cell shape datasets enable significant
86 developments in paleobotany and evolutionary biology.

87 We developed the CuticleTrace toolkit to streamline and automate the tracing and
88 measurement of epidermal pavement cells across a wide variety of taxa, image qualities, and
89 image preparations. Our easily fine-tuned open-source workflow uses the freeware software FIJI
90 (Schindelin et al., 2012) and R Statistical Software (R) (R Core Team, 2022). CuticleTrace
91 generates large cell-shape datasets from images of leaf cuticle or epidermis. Cell-tracing is fast,
92 consistent, and reproduces expert-level measurements.

93

94 METHODS AND RESULTS

95 CuticleTrace description

96 The CuticleTrace workflow consists of four steps. First, users determine appropriate
97 batch-processing inputs with the “Single Image Processor” FIJI macro (Fig. 1b). Second, users
98 batch-process images and measure cells with the “Batch Generate ROIs” and “Batch Measure
99 (Different Scales)” FIJI macros, which generate (1) thresholded and skeletonized binary images
100 (Fig. 1f-g), (2) sets of files recording individual cell shapes known as “regions of interest”
101 (ROIs; Fig. 1i), and (3) shape parameter measurements associated with each ROI (Fig. 1j).
102 Third, resulting cell measurements are filtered with median statistics by the “CuticleTrace Data
103 Filtration” R notebook (Fig. 1k). Last, users can visualize the effects of data filtration with the
104 “Batch Overlay” FIJI macro (Fig. 1j).

105 An illustrated manual for installation and use of FIJI and R tools is available in the
106 supporting information (**Appendix S1**). A video tutorial is available online [link available after

Lloyd et al. – *CuticleTrace: A toolkit for capturing leaf epidermal cell shapes*

107 acceptance] and all software is documented on the CuticleTrace GitHub repository

108 (<https://github.com/benjlloyd/CuticleTrace>).

109 —**Fig. 1 here—**

110 *Determination of batch processing inputs*

111 Both the “Single Image Processor” and “Batch Generate ROIs” macros apply seven user
112 inputs to images. “Single Image Processor” works with an open image, while “Batch Generate
113 ROIs” processes all images in an image set. Each user input sets the parameters for different
114 image processing operations. Before batch-processing, users must first determine the appropriate
115 input parameters on a small subset of images using the “Single Image Processor” macro. The
116 selection of appropriate input parameters is extremely important to ensure accurate results (Fig.
117 2).

118 For both macros, users select:

- 119 1. Whether cell walls are dark on a light background, or light on a dark background
- 120 2. The standard deviation of Gaussian blur (Fig. 1c)
- 121 3. The automated local thresholding algorithm (Fig. 1d, Fig. 2)
- 122 4. The initial local thresholding radius (Fig. 1d)
- 123 5. The range of sizes (in pixels squared) of all cells expected in the image set (Fig. 1d)
- 124 6. The percentage of Fourier descriptors to retain during shape smoothing (Fig. 1e)
- 125 7. The scale (in pixels/unit) of all images in the image set (Fig. 1i)

126 —**Fig. 2 here—**

127 *Image processing and measurement*

128 The “Batch Generate ROIs” macro outputs thresholded and skeletonized binary images,
129 and unfiltered (enhanced and interpolated) ROI sets of all images in a directory (Fig. 1c-i). Users

Lloyd et al. – *CuticleTrace: A toolkit for capturing leaf epidermal cell shapes*

130 may also elect to output measurements of ROI shape parameters if all images have the same
131 scale, or use “Batch Measure (Different Scales)” to measure ROIs of images with differing
132 scales (Fig. 1j, Table 1). These unfiltered ROI sets and measurement files may then be brought
133 directly into the “CuticleTrace Data Filtration” R Notebook for statistical filtration.

134 —**Table 1 here**—

135 *Data filtration*

136 The ROIs produced by the CuticleTrace FIJI analysis pipeline will inevitably include
137 partial cells, multiple cells, vein cells, or non-cuticle image artifacts (e.g., slide background,
138 debris). The “CuticleTrace Data Filtration” R notebook removes these erroneous data points by
139 excluding ROIs with measurements outside one or two median absolute deviations (MADs)
140 from each image’s median area, perimeter, circularity, aspect ratio, roundness, and solidity
141 (Table 1). The notebook then creates new ROI sets of the remaining ROIs post-filtering (Fig. 3).

142 We use the median as our reference point, as unfiltered measurements are non-normally
143 distributed (Fig. 4). This approach retains ROIs that capture the central tendency of each
144 specimen’s epidermal pavement cell morphology.

145 —**Fig. 3 here**—

146 *Data visualization*

147 The “Batch Overlay” FIJI macro allows users to visualize CuticleTrace outputs by
148 creating images overlain with outlines of each ROI in an ROI set, formatted to the user’s
149 preference. “Batch Overlay” may be used to overlay any batch of ROI sets on any batch of
150 images. In our evaluation, we used “Batch Overlay” to visually check the accuracy of ROIs
151 resulting from different input parameters (Fig. 2) and to compare unfiltered ROI sets with the
152 filtered versions from the “CuticleTrace Data Filtration” R Notebook (Fig. 3, 4).

Lloyd et al. – *CuticleTrace: A toolkit for capturing leaf epidermal cell shapes*

153 —Fig. 4 here—

154

155 **CuticleTrace evaluation**

156 We evaluated CuticleTrace across a range of image resolutions, magnifications, and
157 qualities, using an image set of 50 vouchered herbarium specimens from the Cuticle Database
158 (cuticledb.eesi.psu.edu, Barclay et al., 2007). Images were chosen to maximize taxonomic
159 breadth (48 species, 37 genera, 20 families) and span the range of cell shapes and sizes (Fig.
160 S2).

161 We compared CuticleTrace to alternate measurement methods in two ways. We
162 generated CuticleTrace measurements following the protocol outlined in Appendix S1, with user
163 inputs specified in Table 2. First, we compared CuticleTrace measurements (at the $\pm 1\text{MAD}$ and
164 $\pm 2\text{MAD}$ filtering levels) to hand-traced outlines of ten cells followed Dunn et al. (2015), traced
165 by an expert (R.E.D) and University of Wyoming undergraduates (A.I.M, K.S.); and
166 measurements generated by alternate automated methods (LeafNet (Li et al., 2022) and
167 PaCeQuant (Möller et al., 2017)). PaCeQuant did not successfully segment our light-microscopy
168 images (unsurprising, as it was developed for confocal microscopy images), and was excluded
169 from statistical comparisons of segmentation methods.

170 Second, we manually reduced our CuticleTrace and expert datasets to only include the
171 same cells (447 cells across all 50 images). We then completed a one-to-one comparison of
172 CuticleTrace and expert measurements across all images, controlling for cell selection and
173 sample size.

174 —Table 2 here—

175

Lloyd et al. – *CuticleTrace: A toolkit for capturing leaf epidermal cell shapes*

176 *Whole image comparison*

177 The expert outlines served as our evaluation benchmark. We ran a one-way Analysis of
178 Variance (ANOVA) with post-hoc nonparametric Games-Howell analysis for each shape
179 parameter for each image. We selected the Games-Howell test due to differing sample sizes
180 between the four sets of measurements. We used CuticleTrace’s “Batch Overlay” macro to
181 visually compare CuticleTrace and expert tracings (**Fig. S2**).

182 Our analyses showed 100% statistical agreement between CuticleTrace measurements (at
183 both $\pm 1\text{MAD}$ and $\pm 2\text{MAD}$ filtering levels) and expert measurements of area, perimeter, Feret’s
184 diameter, aspect ratio, and roundness (Fig. 5). We observed some variability in circularity,
185 solidity and UI measurements, which was expected due to their sensitivity to small tracing
186 differences. CuticleTrace measurements consistently aligned more closely with expert
187 measurements than expert measurements did with student and LeafNet measurements (Table 3).

188 —**Fig. 5 here**—

189 —**Table 3 here**—

190 *Cell-to-cell comparison*

191 Our cell-to-cell comparison of CuticleTrace and expert measurements of individual cells
192 (447 cells across all 50 images), which showed broad agreement across all shape parameters
193 (Fig. 6). In only 11 of 400 image measurements (50 images, eight shape parameters) were values
194 significantly different at the 2-sigma level—a 2.75% error rate. Seven of the 11 significant
195 differences are concentrated in three images—FLMNH00178 (*Damburneya salicifolia*),
196 FLMNH00561 (*Gleditsia triacanthos*), and FLMNH05215 (*Pouteria durlandii*) (Fig. 6).
197 However, overall, differences between expert and CuticleTrace tracings of the same cells were

Lloyd et al. – *CuticleTrace: A toolkit for capturing leaf epidermal cell shapes*

198 small, and CuticleTrace tracings were reasonable and consistent even when they differed from
199 expert tracings.

200 —**Fig. 6 here—**

201

202 Accuracy of CuticleTrace Measurements

203 Across the wide range of cell shapes and image qualities encapsulated in our test dataset
204 (**Fig. S2**), CuticleTrace produces cell shape measurements that are statistically identical to
205 expert measurements across all shape parameters in most instances, at both the $\pm 1\text{MAD}$ and
206 $\pm 2\text{MAD}$ filtering level. The limited, often non-significant, differences between expert and
207 CuticleTrace measurements may be attributed to two sources of variation. First, the set of cells
208 outlined by CuticleTrace may differ from those traced by an expert in the same image. However,
209 *CuticleTrace* generates a much larger cell measurement dataset than is possible by hand.
210 Therefore, provided the cells selected by CuticleTrace are representative of the whole image, the
211 differences between the two methods were more likely a result of bias in the hand-drawn cells,
212 as the grid-selection method of hand tracing results in smaller sample sizes and tends to favor
213 larger cells.

214 Second, CuticleTrace may emphasize different aspects of cell morphology than an
215 expert. Crenulated cells with obvious three-dimensional morphology showed the greatest
216 number of disagreements (Fig. 6a, 6d). In these images, the expert chose to outline the cell wall
217 at an alternate focal level from the CuticleTrace macros. The choice of focal level is somewhat
218 subjective, however, and CuticleTrace’s interpretation of the cell outline was largely reasonable
219 and consistent. Our cell-to-cell comparison of 447 individual cells across 50 images showed that

Lloyd et al. – *CuticleTrace: A toolkit for capturing leaf epidermal cell shapes*

220 expert and CuticleTrace measurements are highly correlated (Fig. 6). For most images,
221 CuticleTrace and expert measurements were effectively interchangeable.

222 The ease of data visualization built into CuticleTrace with the “Batch Overlay” and
223 “Single Image Processor” macros is an important feature for ensuring accurate cell tracing and
224 ROI filtering. Our design makes qualitative assessment of outputs easy, so that users can
225 visually check all CuticleTrace outputs—thresholded images, skeletonized images, and filtered
226 and unfiltered ROI sets—and modify input parameters as necessary. Additionally, CuticleTrace
227 users may modify the “CuticleTrace Data Filtration” R notebook to suit their needs, and ROI
228 sets may always be manually revised in FIJI.

229 Slide preparation, image quality, and CuticleTrace input parameters were the most
230 important factors in ensuring accuracy in automated measurements. While we intentionally
231 included a wide range of image qualities in our dataset (**Fig. S2**), we did not attempt to analyze
232 Cuticle Database images that were of very poor quality. CuticleTrace’s flexibility allows it to be
233 fine-tuned for a wide variety of image preparations and resolutions, but that same flexibility may
234 lead to ineffective or inaccurate image characterization if users neglect to carefully select input
235 parameters (Fig. 2). It is imperative that users closely follow instructions in the CuticleTrace
236 User Manual (**Appendix S1**).

237

238 **Comparison to Alternate Automated Methods**

239 CuticleTrace is a unique addition to the suite of available methodologies for
240 automatically segmenting and characterizing leaf epidermal morphology. Other approaches—
241 PaCeQuant (Möller et al., 2017) and LeafNet (Li et al., 2022)—also automate epidermal
242 pavement cell segmentation, with some limitations. Many other methods focus on stomata

Lloyd et al. – *CuticleTrace: A toolkit for capturing leaf epidermal cell shapes*

243 detection and characterization (e.g. Fetter et al., 2019; Li et al., 2022). Additional methods have
244 been developed to trace cells in other plant tissues (Wolny et al., 2020) and more generally
245 (Stringer et al., 2021).

246 Of these methods, CuticleTrace is the first to effectively trace and measure epidermal
247 pavement cells across a wide variety of taxa, cell morphologies, and image qualities. The
248 customizability of the “Batch Generate ROIs” and “Single Image Processor” FIJI macros allows
249 users to tune CuticleTrace’s settings to work well for their images. Unlike machine-learning
250 approaches to cell segmentation, CuticleTrace does not require training images and can work
251 with a broad range of morphologies with existing FIJI tools. It can therefore be more easily
252 applied to studies involving diverse samples, detrital cuticle, or extinct taxa.

253

254 CONCLUSIONS

255 The modularity and adaptability of the CuticleTrace toolkit hold great potential for its
256 use outside of the immediate scope of this paper. CuticleTrace allows for the interchange of
257 different parts of its analysis pipeline for alternate applications, and we intend for the toolkit to
258 remain in active development. The local thresholding methods employed by CuticleTrace are
259 effective for segmenting epidermal pavement cells in light microscopy images, but alternative
260 segmentation methods (Möller et al., 2017; Wolny et al., 2020; Stringer et al., 2021; Li et al.,
261 2022; Kirillov et al., 2023) can be swapped into the CuticleTrace pipeline as needed for other
262 applications. Other methods of epidermal cell morphological analysis (Möller et al., 2017;
263 Brown and Jordan, 2023) can also utilize CuticleTrace-generated ROIs to measure shape
264 parameters beyond those included within CuticleTrace.

Lloyd et al. – *CuticleTrace: A toolkit for capturing leaf epidermal cell shapes*

265 CuticleTrace's current inability to detect and mask stomata limits its use on stomata-rich
266 abaxial cuticle, but the toolkit's modular structure is conducive to the integration of machine-
267 learning-based methods for stomatal recognition and masking (Fetter et al., 2019; Aono et al.,
268 2021; Li et al., 2022; Sai et al., 2023), which would further its applicability to abaxial leaf
269 cuticle. With potential for integration with other methods and software, CuticleTrace represents
270 a robust foundation for image binarization, ROI generation, and morphological analysis that
271 may find other applications in plant science.

272 The leaf epidermis contains a wealth of information about plants' evolutionary history
273 and growth environments, and CuticleTrace makes that information significantly more
274 accessible. In both living and fossil plants, epidermal pavement morphology can be utilized to
275 gain insight into plant physiology, ecology, and evolution, and fossil evidence of epidermal cells
276 are integral to some paleoenvironmental studies. The largest barrier to big-data approaches to
277 these questions is the non-trivial task of accurately segmenting epidermal cell images.
278 CuticleTrace represents a significant advance, greatly lowering the barrier to high-throughput
279 studies of epidermal morphology by increasing the consistency of epidermal cell measurements
280 and by vastly decreasing the labor investment required to generate cell shape datasets.

281 ACKNOWLEDGEMENTS

282 RSB acknowledges financial support from NSF grant EAR:1805228. SWP acknowledges
283 support from a 2022 University of Illinois National Center for Supercomputing Applications
284 (NCSA) Faculty Fellowship. EDC, RED, KS, and AIM acknowledge support from NSF grant
285 EAR:145031. BAL acknowledges financial support from Caroline Strömborg and thanks her,
286 Alex Lowe, and Elena Stiles for constructive discussion.

Lloyd et al. – *CuticleTrace: A toolkit for capturing leaf epidermal cell shapes*

287 AUTHOR CONTRIBUTIONS

288 BAL, RSB, RED and SWP conceived the study. BAL conducted the data analysis and created
289 the FIJI image processing macros and ‘R’ filtering code. RED, KS, and AIM provided manual
290 cell outlines. RED and EDC recruited and supervised the University of Wyoming students. BAL
291 and SWP wrote the manuscript with help from RSB and RED. RSB and SWP supervised and
292 directed the research.

293 DATA AVAILABILITY

294 All generated and analyzed data from this study are included in the published article and its
295 Supporting Information (**Fig. S2**). The code for the FIJI macros as well as the R notebook for
296 filtering cells is available in the GitHub repository: (<https://github.com/benjlloyd/CuticleTrace>).

297 REFERENCES

- 298 Aono, A. H., J. S. Nagai, G. da S. M. Dickel, R. C. Marinho, P. E. A. M. de Oliveira, J. P. Papa,
299 and F. A. Faria. 2021. A stomata classification and detection system in microscope
300 images of maize cultivars. *PLOS ONE* 16: e0258679.
- 301 Barclay, R., J. McElwain, D. Dilcher, and B. Sageman. 2007. The Cuticle Database: Developing
302 an interactive tool for taxonomic and paleoenvironmental study of the fossil cuticle
303 record W. *CFS Courier Forschungsinstitut Senckenberg* 258: 39–55.
- 304 Brown, M. J. M., and G. J. Jordan. 2023. No cell is an island: characterising the leaf epidermis
305 using epidermalmorph, a new R package. *New Phytologist* 237: 354–366.
- 306 Bush, R. T., J. Wallace, E. D. Currano, B. F. Jacobs, F. A. McInerney, R. E. Dunn, and N. J.
307 Tabor. 2017. Cell anatomy and leaf δ¹³C as proxies for shading and canopy structure in
308 a Miocene forest from Ethiopia. *Palaeogeography, Palaeoclimatology, Palaeoecology*
309 485: 593–604.
- 310 Dunn, R. E., C. A. E. Strömberg, R. H. Madden, M. J. Kohn, and A. A. Carlini. 2015. Linked
311 canopy, climate, and faunal change in the Cenozoic of Patagonia. *Science* 347: 258–261.

Lloyd et al. – *CuticleTrace: A toolkit for capturing leaf epidermal cell shapes*

- 312 Fetter, K. C., S. Eberhardt, R. S. Barclay, S. Wing, and S. R. Keller. 2019. StomataCounter: a
313 neural network for automatic stomata identification and counting. *New Phytologist* 223:
314 1671–1681.
- 315 Kirillov, A., E. Mintun, N. Ravi, H. Mao, C. Rolland, L. Gustafson, T. Xiao, et al. 2023.
316 Segment Anything.
- 317 Kürschner, W. M. 1997. The anatomical diversity of recent and fossil leaves of the durmast oak
318 (*Quercus petraea* Lieblein/Q. *pseudocastanea* Goeppert) — implications for their use as
319 biosensors of palaeoatmospheric CO₂ levels. *Review of Palaeobotany and Palynology*
320 96: 1–30.
- 321 Li, S., L. Li, W. Fan, S. Ma, C. Zhang, J. C. Kim, K. Wang, et al. 2022. LeafNet: a tool for
322 segmenting and quantifying stomata and pavement cells. *The Plant Cell* 34: 1171–1188.
- 323 McElwain, J. C., and W. G. Chaloner. 1996. The Fossil Cuticle as a Skeletal Record of
324 Environmental Change. *PALAIOS* 11: 376–388.
- 325 Milligan, J. N., A. G. Flynn, J. D. Wagner, L. L. R. Kouwenberg, R. S. Barclay, B. W. Byars, R.
326 E. Dunn, et al. 2021. Quantifying the effect of shade on cuticle morphology and carbon
327 isotopes of sycamores: present and past. *American Journal of Botany* 108: 2435–2451.
- 328 Möller, B., Y. Poeschl, R. Plötner, and K. Bürstenbinder. 2017. PaCeQuant: A Tool for High-
329 Throughput Quantification of Pavement Cell Shape Characteristics. *Plant Physiology*
330 175: 998–1017.
- 331 R Core Team. 2022. R: A Language and Environment for Statistical Computing. R Foundation
332 for Statistical Computing, Vienna, Austria.
- 333 Royer, D. L. 2001. Stomatal density and stomatal index as indicators of paleoatmospheric CO₂
334 concentration. *Review of Palaeobotany and Palynology* 114: 1–28.
- 335 Sai, N., J. P. Bockman, H. Chen, N. Watson-Haigh, B. Xu, X. Feng, A. Piechatzek, et al. 2023.
336 StomaAI: an efficient and user-friendly tool for measurement of stomatal pores and
337 density using deep computer vision. *New Phytologist* 238: 904–915.
- 338 Schindelin, J., I. Arganda-Carreras, E. Frise, V. Kaynig, M. Longair, T. Pietzsch, S. Preibisch, et
339 al. 2012. Fiji: an open-source platform for biological-image analysis. *Nature Methods* 9:
340 676–682.
- 341 Stringer, C., T. Wang, M. Michaelos, and M. Pachitariu. 2021. Cellpose: a generalist algorithm
342 for cellular segmentation. *Nature Methods* 18: 100–106.
- 343 Strömberg, C. A. E. 2011. Evolution of Grasses and Grassland Ecosystems. *Annual Review of*
344 *Earth and Planetary Sciences* 39: 517–544.

Lloyd et al. – *CuticleTrace: A toolkit for capturing leaf epidermal cell shapes*

- 345 Vőfély, R. V., J. Gallagher, G. D. Pisano, M. Bartlett, and S. A. Braybrook. 2019. Of puzzles
346 and pavements: a quantitative exploration of leaf epidermal cell shape. *New Phytologist*
347 221: 540–552.
- 348 Wolny, A., L. Cerrone, A. Vijayan, R. Tofanelli, A. V. Barro, M. Louveaux, C. Wenzl, et al.
349 2020. Accurate and versatile 3D segmentation of plant tissues at cellular resolution. *eLife*
350 9: e57613.
- 351 Zhao, C., Y. Zhang, J. Du, X. Guo, W. Wen, S. Gu, J. Wang, and J. Fan. 2019. Crop Phenomics:
352 Current Status and Perspectives. *Frontiers in Plant Science* 10.

353

Lloyd et al. – *CuticleTrace: A toolkit for capturing leaf epidermal cell shapes*

354 **TABLES**

355 **Table 1. Descriptions or equations of all shape parameters measured by CuticleTrace.**

Measurement Parameter	Description or Equation
Area	The area of an ROI.
Perimeter	The length of the outside boundary of an ROI.
Bounding Rectangle	The X-Y coordinates and dimensions of the smallest rectangle that encloses an ROI.
Fit Ellipse	The dimensions and orientation of an ellipse fit to an ROI.
Feret's Diameter	The longest distance between any two points on the ROI boundary.
Minimum Feret's Diameter	The shortest distance between any two points on the ROI boundary.
Circularity	$4\pi * \frac{[Area]}{[Perimeter]^2}$
Aspect Ratio	$\frac{[Major\ Axis\ of\ Fit\ Ellipse]}{[Minor\ Axis\ of\ Fit\ Ellipse]}$
Roundness	$4 * \frac{[Area]}{\pi * [Major\ Axis\ of\ Fit\ Ellipse]^2}$
Solidity	$\frac{[Area]}{[Area\ of\ Convex\ Hull]}$
Undulation Index	$\frac{[Perimeter]}{2\pi * \sqrt{[Area]/\pi}}$

356

357 **Table 2. CuticleTrace batch-processing inputs for our 50-image test dataset.**

Input Parameter	Value
Cell Walls on Background	Dark on Light
Gaussian Blur σ	2 pixels
Thresholding Algorithm	Sauvola (Sauvola & Pietikäinen, 2000)
Initial Thresholding Radius	50 pixels
ROI Size Filter	500-50,000 pixels ²
Smoothing Value	5% of Fourier descriptors

358

359

Lloyd et al. – *CuticleTrace: A toolkit for capturing leaf epidermal cell shapes*

360
361
362
363

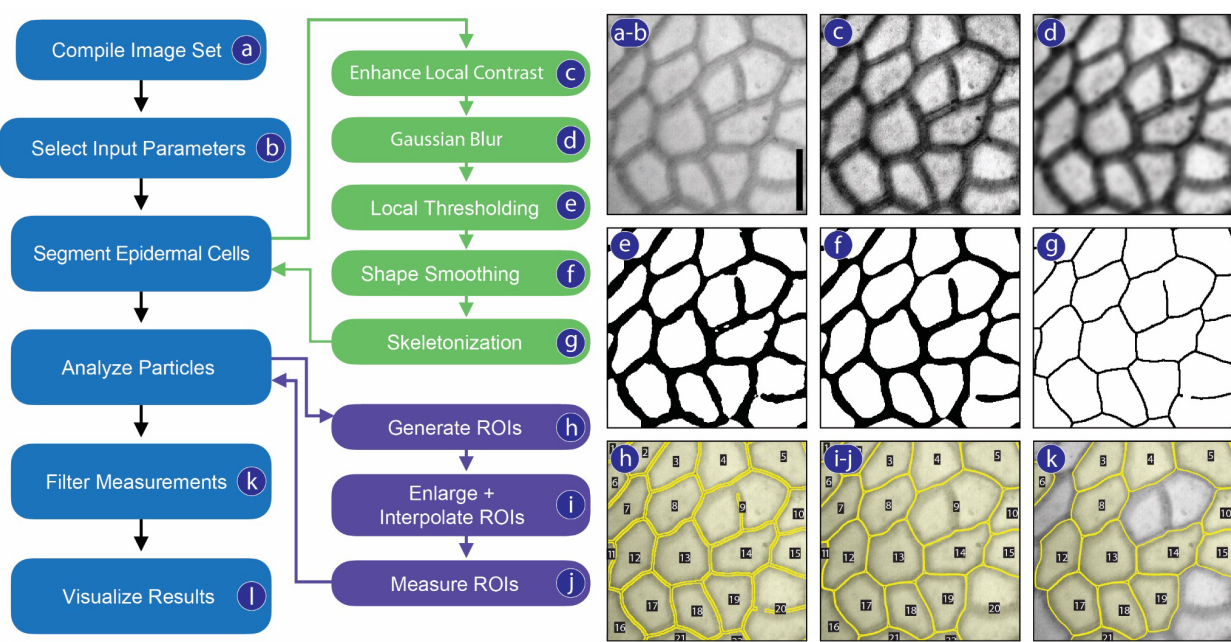
Table 3. Statistical evaluation of $\pm 1\text{MAD}$ and $\pm 2\text{MAD}$ CuticleTrace measurements, student measurements, and LeafNet measurements, in comparison to expert measurements.

Shape Parameter	Average Games-Howell p-value in comparison to Expert					% of measurements statistically identical to Expert (p-values $> .05$)				
	CuticleTrace					CuticleTrace				
	$\pm 1\text{MAD}$	$\pm 2\text{MAD}$	Cell to Cell	Student	LeafNet	$\pm 1\text{MAD}$	$\pm 2\text{MAD}$	Cell to Cell	Student	LeafNet
Area	0.85	0.89	0.56	0.74	0.55	100	100	100	94	84
Perimeter	0.82	0.82	0.68	0.54	0.60	100	100	100	86	82
Feret's	0.85	0.88	0.64	0.66	0.72	100	100	100	94	88
Diameter										
Circularity	0.52	0.53	0.44	0.31	0.06	78	82	94	58	12
Aspect Ratio	0.79	0.82	0.88	0.75	0.81	100	100	100	100	100
Roundness	0.78	0.82	0.88	0.81	0.78	100	100	100	100	100
Solidity	0.44	0.47	0.42	0.34	0.18	76	78	90	72	30
Undulation Index	0.52	0.53	0.44	0.25	0.06	82	88	94	52	12
Mean	0.70	0.72	0.62	0.55	0.47	92.0	93.5	97.3	82.0	63.5

364

365

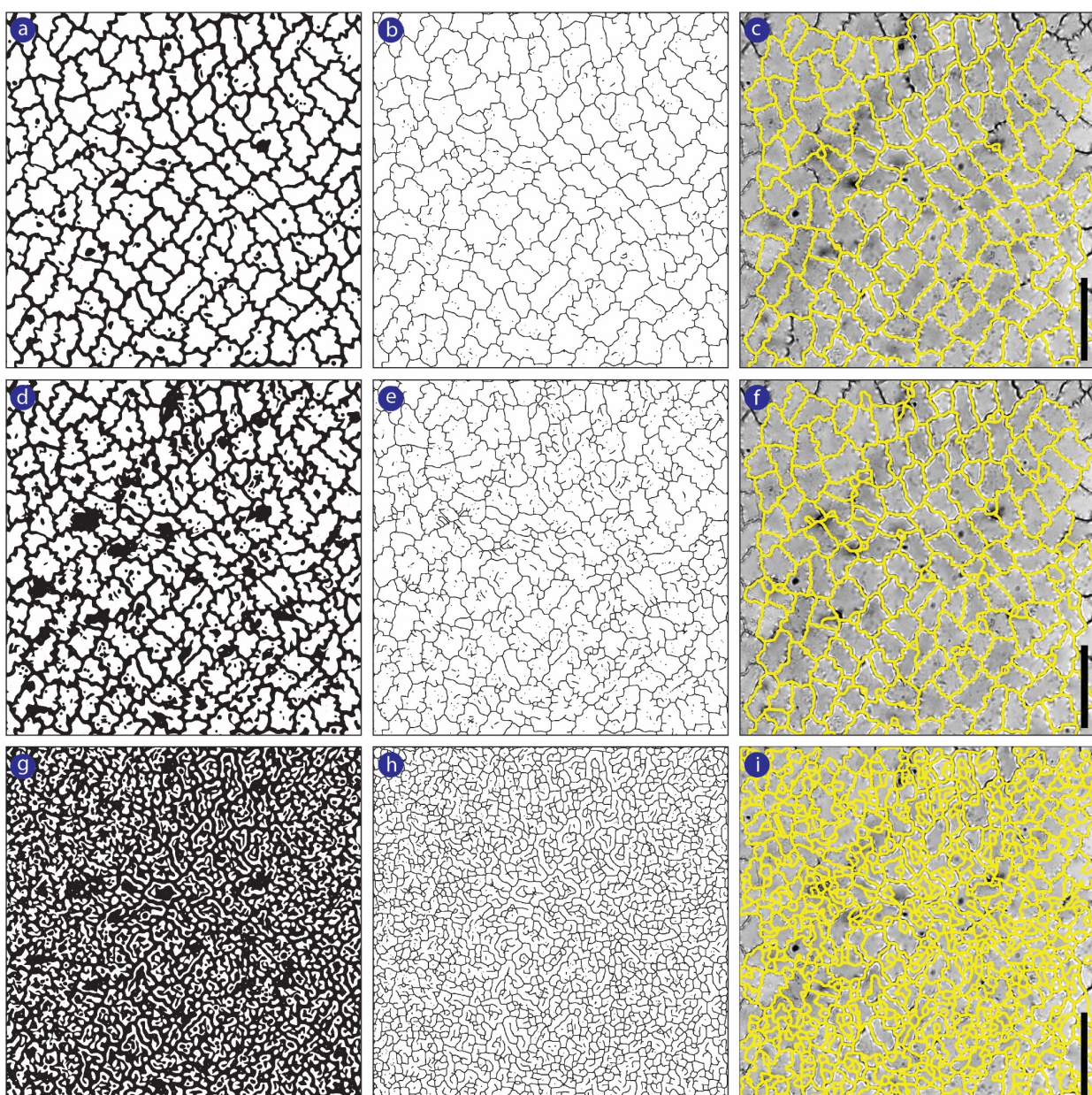
366 **FIGURES**



367
368
369
370
371
372
373
374
375

Fig. 1 Processing workflow for the CuticleTrace toolkit (left), illustrated on an image of *Castanea pumila* (Fagaceae, FLMNH00115). Scale bar is 10 μm . Processing starts by (a) compiling an image set and (b) selecting input parameters. This is followed by epidermal cell segmentation, consisting of (c) local contrast enhancement, (d) Gaussian blur, (e) local thresholding, (f) shape smoothing, and (g) skeletonization. Particles are analyzed in FIJI, by (h) generating ROIs, (i) enlarging and interpolating ROIs, and (j) measuring ROIs. ROI measurements are (k) filtered with median statistics, and (l) visualized overlaying unprocessed images.

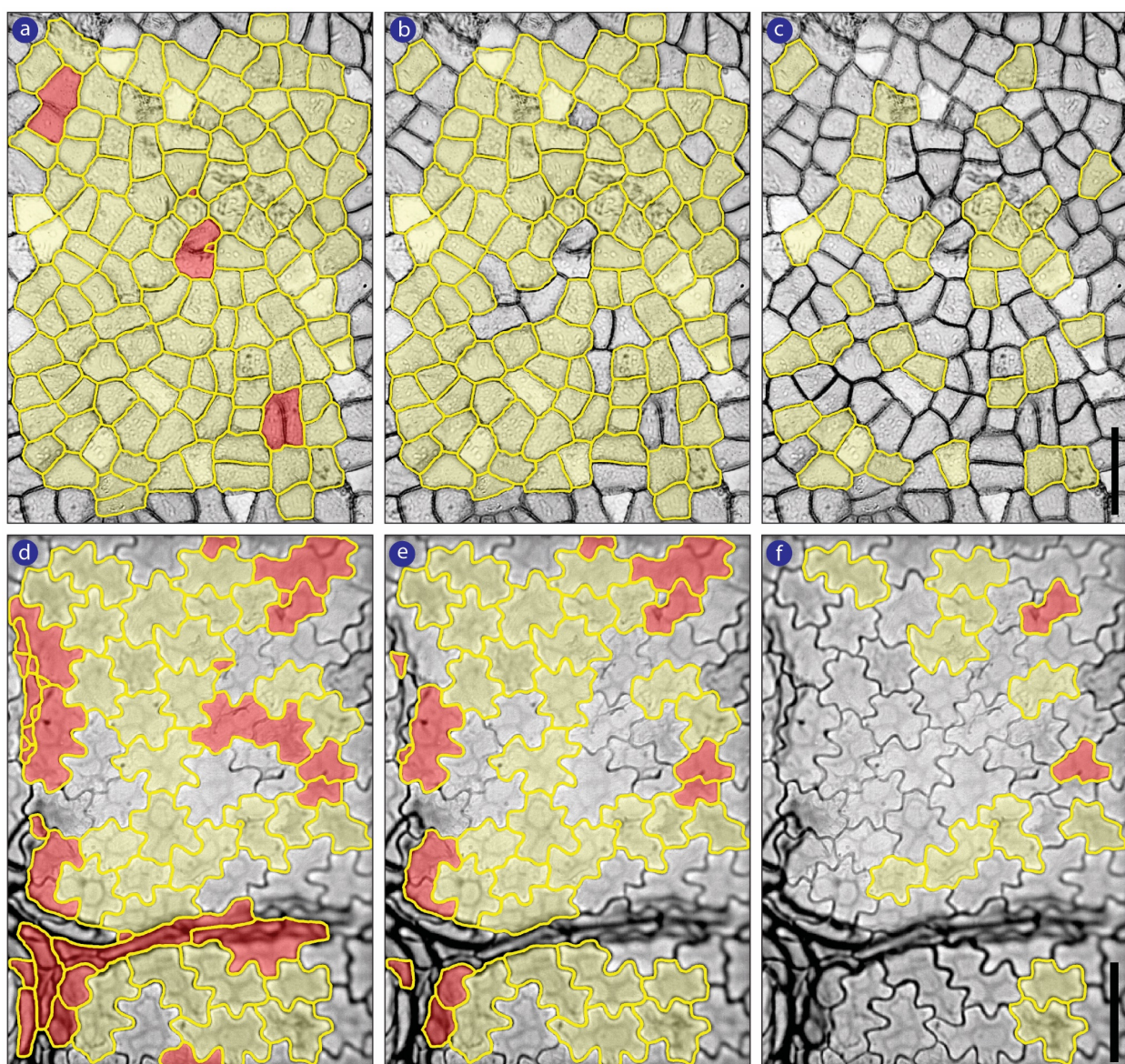
Lloyd et al. – *CuticleTrace*: A toolkit for capturing leaf epidermal cell shapes



376
377
378
379
380
381

Fig. 2 The effect of thresholding (**a, d, g**) on skeletonization (**b, e, h**) and unfiltered ROI sets (**c, f, i**), demonstrated on *Talisia princeps* - Sapindaceae, FLMNH00443. The image is thresholded by (**a-c**) Sauvola local thresholding (ideal), (**d-f**) Bernsen local thresholding (satisfactory), and (**g-i**) NiBlack local thresholding (ineffective). Scale bars are 50 μ m.

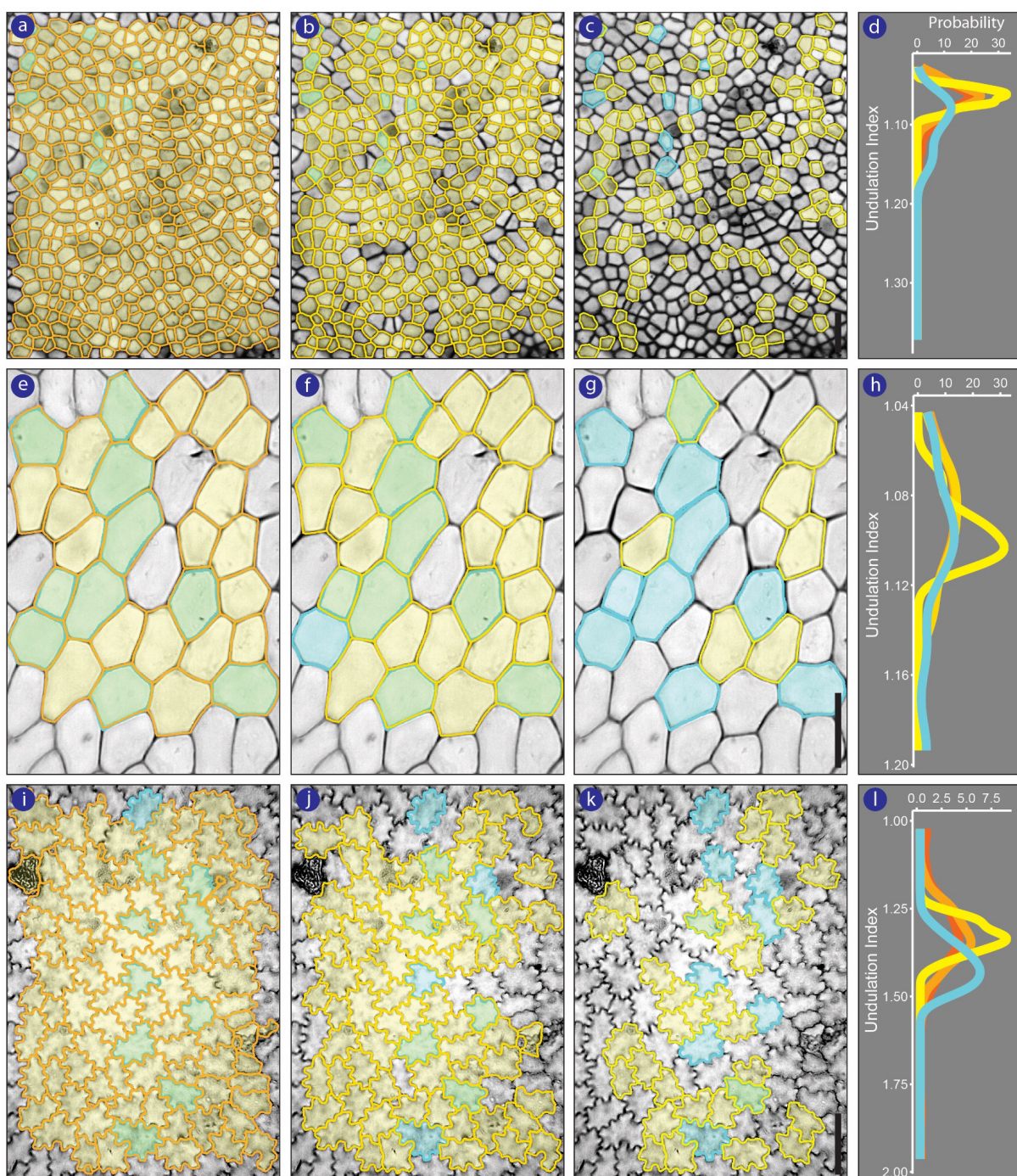
Lloyd et al. – *CuticleTrace: A toolkit for capturing leaf epidermal cell shapes*



382
383
384
385
386
387
388
389

Fig. 3 Removal of unwanted ROIs by filtering with median statistics. **(a-c)** *Ocotea tarapotana* - Lauraceae, FLMNH00185; **(d-f)** *Acer skutchii* - Aceraceae, FLMNH00714. ROI sets that are **(a, d)** unfiltered, **(b, e)** $\pm 2\text{MAD}$ -filtered, and **(c, f)** $\pm 1\text{MAD}$ -filtered. Yellow outlines represent ROIs retained at each filtering level. Yellow-shaded ROIs accurately characterize epidermal pavement cells. Red-shaded ROIs do not accurately characterize pavement cells and are thus not wanted in the final dataset. Scale bars are 50 μm .

Lloyd et al. – CuticleTrace: A toolkit for capturing leaf epidermal cell shapes



390
391
392
393
394
395
396
397
398
399

Fig. 4 CuticleTrace-generated ROI sets (yellow) compared to expert hand drawn ROI sets (cyan), with subsequent filtering using median statistics. Cells with overlapping CuticleTrace and expert-generated ROIs appear green. Columns show ROI sets that are unfiltered (**a-c**) *Nectandra oppositifolia* - Lauraceae, FLMNH00260; (**e-g**) *Guarea bijuga* - Meliaceae, FLMNH00850, and (**i-l**) *Anaxagorea petiolata* - Annonaceae, FLMNH02589. (**d, h, l**) probability density plots showing distributions of Undulation Index values across all 4 datasets for each image; hand-traced - cyan, unfiltered - dark orange, $\pm 2\text{MAD}$ - light orange, $\pm 1\text{MAD}$ - yellow. Scale bars are 50 μm .

Lloyd et al. – *CuticleTrace: A toolkit for capturing leaf epidermal cell shapes*

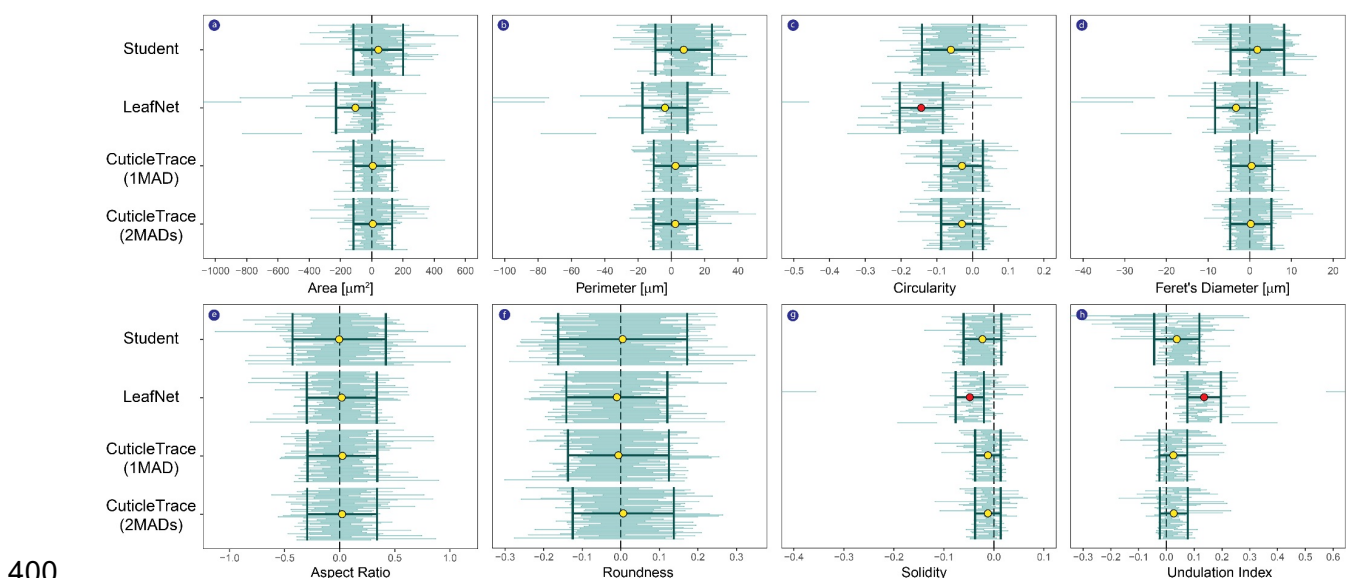
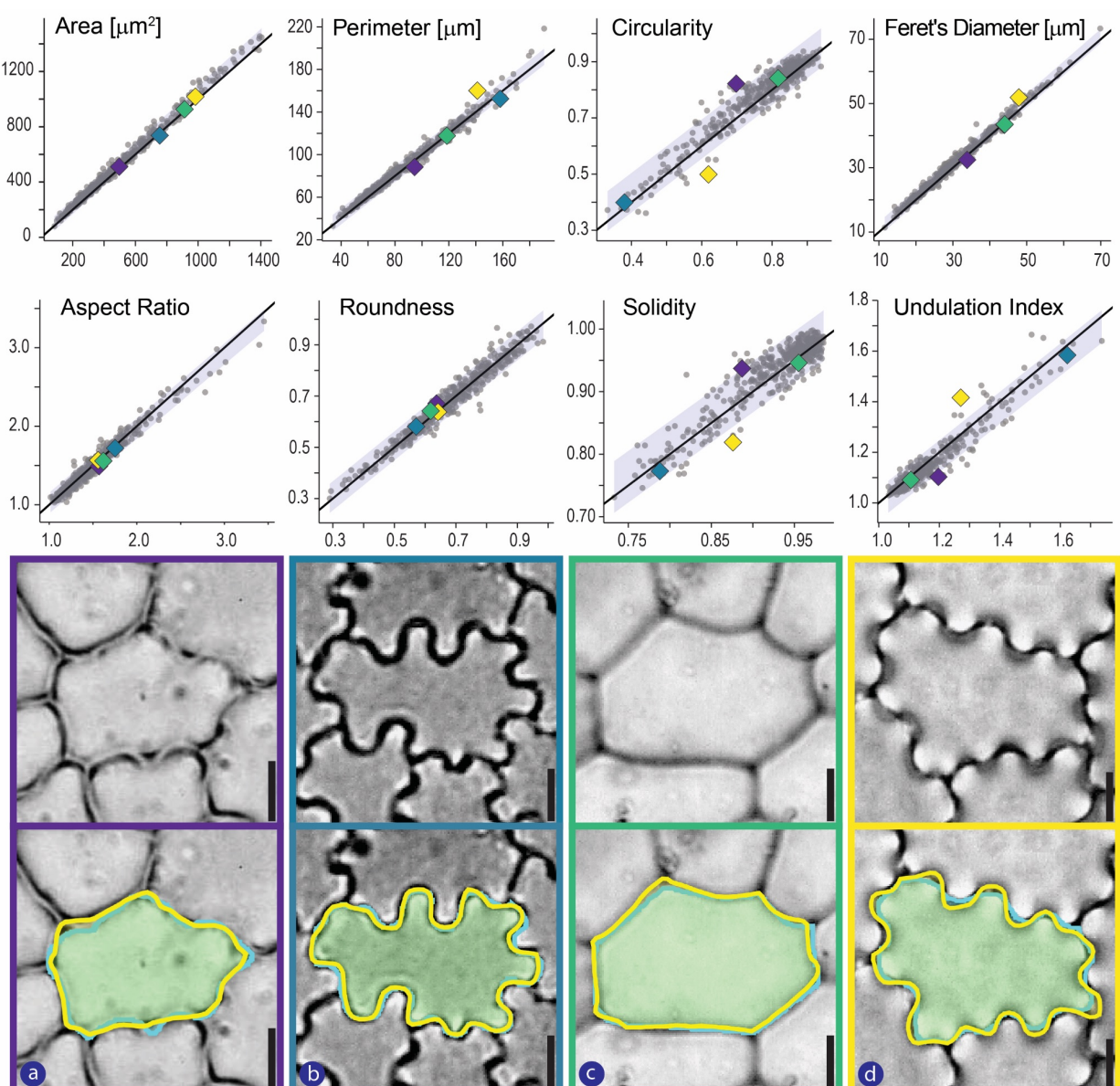


Fig. 5 Post-hoc Games-Howell results for all 50 images, separated by shape parameter.

Comparisons are all relative to the hand-drawn expert results (zero). Student data was also hand-drawn; LeafNet and CuticleTrace are automated methods. Each small horizontal bar represents the 95% confidence interval of the Games-Howell mean difference estimate applied to a single image in the comparative dataset. The image position in the stack is maintained for each shape parameter. Darker bars with center circles are the mean $\pm 2\sigma$ for each of the comparative stacks of Games-Howell results. Yellow center circles are non-significant; red center circles are significantly different from the expert.

Lloyd et al. – *CuticleTrace: A toolkit for capturing leaf epidermal cell shapes*



410
411 **Fig. 6** Cell-to-cell comparison of Expert and CuticleTrace measurements. Upper panel:
412 Correlation between Expert (x-axis) and CuticleTrace (y-axis) measurements across 447 cells
413 and all relevant shape parameters, distributed between 50 images. Black lines have a slope of
414 one, indicating 100% correlation. Shaded areas show 95% prediction intervals. Colored symbols
415 correlate to the four images presented in the lower panel, which provides a visual comparison of
416 the difference between cell outlines hand-drawn by an expert (cyan line) versus the CuticleTrace
417 automated procedure (yellow line). Lower panel: (a) *Gleditsia triacanthos* - Fabaceae,
418 FLMNH00081; (b) *Toxicodendron striatum* - Anacardiaceae, FLMNH00510; (c) *Oreopanax*
419 *capitatus* - Araliaceae, FLMNH00767; (d) *Pouteria durlandii* - Sapotaceae, FLMNH05215.
420 Scale bars are 10 μm .

Lloyd et al. – *CuticleTrace: A toolkit for capturing leaf epidermal cell shapes*

421 **Supporting Information**

422 **Appendix S1** – A detailed illustrated user manual for the CuticleTrace toolkit.

423 **Fig. S2** – Images of ROI outputs from CuticleTrace (Unfiltered, $\pm 1\text{MAD}$, $\pm 2\text{MAD}$) and expert

424 hand-tracing on all 50 images in our test dataset.

425 **ORCID**

426 Richard S. Barclay: <https://orcid.org/0000-0003-4979-6970>

427 Ellen D. Currano: <https://orcid.org/0000-0002-5242-8573>

428 Regan E. Dunn: <https://orcid.org/0000-0002-6042-0619>

429 Benjamin A. Lloyd: <https://orcid.org/0000-0001-6749-2386>

430 Surangi W. Punyasena: <https://orcid.org/0000-0003-2110-5840>